Published OnlineFirst February 14, 2019; DOI: 10.1158/1078-0432.CCR-18-3041

Precision Medicine and Imaging

Clinical Cancer Research

A Variant of a Killer Cell Immunoglobulin-like Receptor Is Associated with Resistance to PD-1 Blockade in Lung Cancer

Marcel P. Trefny[1], Sacha I. Rothschild[1,2], Franziska Uhlenbrock[1], Dietmar Rieder[3], Benjamin Kasenda[2], Michal A. Stanczak[1], Fiamma Berner[4], Abhishek S. Kashyap[1], Monika Kaiser[1], Petra Herzig[1], Severin Poechtrager[5], Daniela S. Thommen[6], Florian Geier[7], Spasenija Savic[8], Philip Jermann[8], Ilaria Alborelli[8], Stefan Schaub[9], Frank Stenner[1,2], Martin Früh[10], Zlatko Trajanoski[3], Lukas Flatz[4], Kirsten D. Mertz[5], Alfred Zippelius[1,2], and Heinz Läubli[1,2]

Abstract

Purpose: PD-(L)1–blocking antibodies have clinical activity in metastatic non–small cell lung cancer (NSCLC) and mediate durable tumor remissions. However, the majority of patients are resistant to PD-(L)1 blockade. Understanding mechanisms of primary resistance may allow prediction of clinical response and identification of new targetable pathways.

Experimental Design: Peripheral blood mononuclear cells were collected from 35 patients with NSCLC receiving nivolumab monotherapy. Cellular changes, cytokine levels, gene expression, and polymorphisms were compared between responders and nonresponders to treatment. Findings were confirmed in additional cohorts of patients with NSCLC receiving immune checkpoint blockade.

Results: We identified a genetic variant of a killer cell immunoglobulin-like receptor (KIR) *KIR3DS1* that is associated with primary resistance to PD-1 blockade in patients with NSCLC. This association could be confirmed in independent cohorts of patients with NSCLC. In a multivariate analysis of the pooled cohort of 135 patients, the progression-free survival was significantly associated with presence of the *KIR3DS1* allele (HR, 1.72; 95% confidence interval, 1.10–2.68; $P = 0.017$). No relationship was seen in cohorts of patients with NSCLC who did not receive immunotherapy. Cellular assays from patients before and during PD-1 blockade showed that resistance may be due to NK-cell dysfunction.

Conclusions: We identified an association of the *KIR3DS1* allelic variant with response to PD-1–targeted immunotherapy in patients with NSCLC. This finding links NK cells with response to PD-1 therapy. Although the findings are interesting, a larger analysis in a randomized trial will be needed to confirm KIRs as predictive markers for response to PD-1–targeted immunotherapy.

Introduction

Adaptive immune escape of tumor cells by upregulation of ligands for programmed death 1 (PD-1) has been identified as an important and targetable pathway in many cancer types (1, 2). Many clinical trials have demonstrated that targeting PD-1 or its ligand PD-L1 with immune checkpoint inhibitors (ICI) can restore antitumor immunity and induce durable remission (1, 2). In patients with non–small-cell lung cancer (NSCLC), several trials have demonstrated a survival benefit with PD-(L)1–blocking antibodies in patients with metastatic (3–7) and locally advanced NSCLC (8). Yet, most patients have primary resistance to PD-(L)1 blockade: approximately 20% to 25% of unselected patients with NSCLC achieve an objective response while 40% to 50% have progressive disease. Understanding mechanisms of primary resistance to PD-(L)1 blockade is important in the search for potentially targetable pathways and may ultimately allow discrimination between patients that derive benefit from PD-(L)1 blockade and those requiring combination strategies or alternative treatment approaches.

Different mechanisms of primary and acquired resistance to PD-(L)1 blockade have been described, including defects in human leukocyte antigen (HLA) class I presentation, cellular

[1]Laboratory of Cancer Immunology, Department of Biomedicine, University Hospital and University of Basel, Basel, Switzerland. [2]Department of Internal Medicine, Division of Oncology, University Hospital Basel, Basel, Switzerland. [3]Biocenter, Division of Bioinformatics, Medical University of Innsbruck, Innsbruck, Austria. [4]Institute of Immunobiology and Oncology, Cantonal Hospital St. Gallen, St. Gallen, Switzerland. [5]Cantonal Hospital Liestal, Liestal, Switzerland. [6]Division of Molecular Oncology and Immunology, Oncode Institute, The Netherlands Cancer Institute, Amsterdam, the Netherlands. [7]Department of Biomedicine, Division of Bioinformatics, University Hospital and University of Basel, Basel, Switzerland. [8]Institute of Pathology, University Hospital Basel, Basel, Switzerland. [9]HLA-Diagnostic & Immunogenetics, Department of Laboratory Medicine, University Hospital Basel, Basel, Switzerland. [10]Department of Medical Oncology/Hematology, Cantonal Hospital of St. Gallen, St. Gallen and University of Bern, Bern, Switzerland.

Note: Supplementary data for this article are available at Clinical Cancer Research Online (http://clincancerres.aacrjournals.org/).

M.P. Trefny and S.I. Rothschild contributed equally to this article.

A. Zippelius and H. Läubli equally supervised the work.

Corresponding Authors: Heinz Läubli, University Hospital of Basel, Petersgraben 4, Basel 4031, Switzerland. Phone: 416-1265-5074; Fax: 416-1265-5316; E-mail: heinz.laeubli@unibas.ch; and Alfred Zippelius, E-mail: alfred.zippelius@usb.ch

doi: 10.1158/1078-0432.CCR-18-3041

Published OnlineFirst February 14, 2019; DOI: 10.1158/1078-0432.CCR-18-3041

Translational Relevance

Only a minority of patients with NSCLC respond to anti–PD-(L)1 therapy. The identification of resistance mechanisms to anti–PD-(L)1 therapy can identify biomarkers of response and potential new targets for cancer immunotherapy. Here, we identify an allelic variant of an NK-cell receptor to be associated with resistance to PD-1–targeted immunotherapy in NSCLC. On the basis of this finding, further exploratory analyses show that NK cells might be potential mediators of resistance to PD-1–blocking antibodies. The described KIR variant is not associated with outcome differences in patients undergoing chemotherapy for stage IV or in the potentially curative setting of stage I–III disease.

adaptation of the tumor microenvironment, low mutational burden, and mutations or defects in the IFNγ pathway (9). To date, most of the focus of investigations has been on how T cells interact with tumor cells, while other immune cells may be critical as well. Recently, cross-talk between natural killer (NK) and dendritic cells has been associated with response to PD-1 blockade in melanoma (10). In this study, we aimed to identify mechanisms of resistance and potential new targetable pathways in patients with metastatic NSCLC that received PD-1 blockade using a comprehensive analysis of peripheral blood from responding and nonresponding patients. We found that the allelic variant *KIR3DS1* is associated with primary resistance to PD-1 blockade and is mainly expressed on NK cells. *KIR3DS1* is an alternative allele at the *KIR3DL1* locus coding for an activating receptor unlike the *KIR3DL1* alleles that encode for inhibitory receptors. *KIR3DS1* mainly differs from *KIR3DL1* in its signaling binding domains at the cytoplasmic tail (11). In addition, peripheral NK-cell reactivity is enhanced in patients responding to PD-1 blockade, suggesting that NK cells are involved in response to immunotherapy.

Materials and Methods

Patients and sample preparation

Serum and peripheral blood mononuclear cells (PBMC) were prospectively collected from 35 patients with metastatic NSCLC (discovery cohort) immediately before the first administration and after two cycles (week 4) of treatment with PD-1 blockade at the University Hospital Basel (Basel, Switzerland). All patients that were planned for immunotherapy after progression on chemotherapy were asked to participate. Ethics approval was obtained from the local ethical committee to analyze the tissue and blood samples (Ethikkomission Nordwestschweiz, EK321/10) and written informed consent was obtained from all patients prior to sample collection in accordance with the Declaration of Helsinki. Objective radiologic response was determined by RECIST 1.1 by a thoracic radiologist, with scans performed every 6–8 weeks. Single-cell suspensions of primary NSCLC tumor samples were prepared by digestion after surgical removal.

For validation and comparison, we examined whole-exome sequencing data from a previously published cohort of patients with metastatic NSCLC treated with pembrolizumab (12). In addition, we examined a third independent cohort of patients from St. Gallen with NSCLC with PD-(L)1 inhibitors by PCR (approved by the local ethical committee, Ethikkommission Ostschweiz, EKOS). Finally, early-stage NSCLCs in the TracerX study cohort not treated with immunotherapy were analyzed by whole-exome sequencing (13).

Cell lines

The K562 cell line (ATCC CCL-243) was received from the ATCC in 2010. Cells were confirmed to be negative for *Mycoplasma* by PCR as described (14) after every freeze–thaw cycle and then passaged every 2–3 days for a maximum of 10 passages.

Multicolor flow cytometry

PBMCs were isolated as published previously (15). Multicolor flow cytometry was performed after staining dead cells with Live/Dead Zombie UV and various panels of antibodies (see Appendix p 2). Corresponding isotype antibodies were used as controls. Tumor samples were analyzed by flow cytometry with a Fortessa LSR II flow cytometer (BD Biosciences). For intracellular cytokine staining, cells were fixed and permeabilized using IC-Fixation or Fix/Perm Kit (eBioscience). For RNA sample collection, peripheral $CD8^+$ T cells were sorted by fluorescence-activated cell sorting using a BD FACS Aria III.

Molecular analysis of *KIR3DS1/L1* and *HLA* locus

The *KIR3DS1/L1* locus was analyzed from germline DNA isolated from peripheral blood by PCR as described previously (16). The *HLA-A*, *-B*, and *-C* were typed by molecular methods (FluoGene;Inno-train) and the presence of Bw4 and Bw6 within the *HLA-A* and *HLA-B* determined.

Bioinformatic analysis of *KIR3DS1/L1* and *HLA* status from whole-exome sequencing data

To identify polymorphisms and genetic variants in *KIR* alleles from whole-exome sequencing data, germline whole-exome sequencing data from the TracerX dataset EGAD00001003206 was obtained under a data access agreement through the European Genome Archive (https://ega-archive.org). Sequence alignments were first sorted by read name using SAMtools 1.3.1 (17) and separated into paired FASTQ files using picard 2.9.2 (http://broadinstitute.github.io/picard). Parts of the KIR genome region (GRCh37; *KIR3DL1* ± 100bp chr19:55327793-55342333, *KIR3DS1* ± 100bp chr19_gl000209_random:69997-84758) were extracted from the provided sequence alignments using SAMtools 1.3.1. We used BLAST to identify three unique sequence regions distinguishing *KIR3DS1/L1* (Supplementary Data). We then used featureCounts (18) to quantify the number of sequencing reads from each individual normal sample aligning to these three distinguished regions (primary, concordant paired-end alignments, having >90% region overlap, and no CIGAR operations). We calculated the LogR ratio for the individual counts and used these measures to assess the *KIR3DS1/L1* genotype (the script for the analysis is deposited at https://github.com/mui-icbi/KIRcaller). We used the "Pushing Immunogenetics to the Next Generation" (PING) method developed by Norman and colleagues (19) in an independent cohort (TracerX) to cross-validate the genotyping of the *KIR* alleles.

RNA sequencing and analysis

Library was constructed with the Illumina TruSeq Nano Kit and sequenced with the Illumina HiSeq 3000. Reads were aligned to the UCSC hg19 version of the human genome using the spliced

Published OnlineFirst February 14, 2019; DOI: 10.1158/1078-0432.CCR-18-3041

read aligner STAR (2.5.1). The R/Bioconductor package QuasR (version 1.10.1, R version 2.3.4) was used to assess read and alignment quality. Gene expression was quantified by the qCount function of QuasR using an exon-union model of hg19 RefSeq genes (downloaded from UCSC 2015-02-09). The R package edgeR was used for differential gene expression analysis. For within time-point comparisons, a linear model including the combined factor "response" and "time" was fitted to the raw counts using function glmFit and differential expression between responders [i.e., partial response (PR) according to RECIST 1.1 criteria] and nonresponders [i.e., progressive disease (PD) by RECIST 1.1] at time points before and during treatment were evaluated by a likelihood ratio test using function glmLRT from edgeR. *P* values were adjusted by controlling the FDR. For within-response group comparisons, a second model including the factor "patient id" was fitted and the differential temporal effects between both groups were evaluated by likelihood ratio tests. The results of the RNA sequencing have been deposited on Gene Expression Omnibus (GEO, https://www.ncbi.nlm.nih.gov/geo) under the number GSE111414.

TML NGS library preparation and sequencing

The Oncomine Tumor Mutation Load Assay (TML assay) is a PCR-based next-generation sequencing assay. The panel covers 1.7 megabases (Mb) of 409 genes that are associated with cancer. The panel consists of 15,513 primer pairs that are evenly distributed in two pools. The genomic regions covered by the panel are divided into 1.2 Mb of exonic and 0.45 Mb of intronic sequences.

Utilizing Ion AmpliSeq library preparation technology, library preparation requires only 20 ng of input DNA (10 ng/primer pool) extracted from formalin-fixed, paraffin-embedded cancer specimens. Briefly, a multiplex PCR is performed to amplify the target regions in the genome. The primer sequences are then digested from the ends of the PCR products using a proprietary enzyme (Thermo Fisher Scientific). Finally, barcoded sequencing adapters are ligated to the enriched targets, and the final libraries are cleaned up using AmpureXP beads (Agencourt). Template preparation was performed on an Ion Chef instrument and the loaded 540 chips were sequenced on an Ion S5 Semiconductor Sequencer (Thermo Fisher Scientific). Minimal coverage (>500×) and uniformity (>90%) values were used to ensure that only high-quality data were used for downstream analysis.

Reads were aligned to the hg19 reference genome using Torrent Suite Software 5.8 and BAM files were transferred to Ion Reporter Software 5.6 for variant calling and secondary analysis including tumor mutation burden (TMB) calculation.

TML score calculation

TMB was calculated using TML analysis workflow "Oncomine Tumor Mutation Load – w1.1" on the Ion Reporter Software v5.6. Mutation load using this workflow is defined as nonsynonymous and synonymous somatic mutations per covered megabases, including missense and nonsense point mutations.

Briefly, after variant calling, variants were filtered by a minimal allelic frequency of 10% and germline variants were removed: variant alleles present from the 1,000 Genome Project, NHLBI GO Exome Sequencing Project, and Exome Aggregation Consortium were filtered out. The remaining somatic variants were the used to calculate the TMB value by dividing the number of variants by the number of covered megabases.

NK cell degranulation and cytotoxicity assay

Whole-bulk PBMCs containing NK cells from patients with NSCLC before and during PD-1 blockade treatment were thawed. A total of 1×10^4 K562 target cells were cocultured with 2×10^5 PBMCs (effector to target ratio 20:1) in the presence of fluorochrome-coupled anti-CD107a antibody. After 1 hour of coincubation, Monensin and Brefeldin were added to the culture to accumulate cytokines intracellularly. After 5 hours of additional coincubation, the cells were fixed and stained for IFNγ and TNFα. The samples were then analyzed by flow cytometry gated on $CD56^+$ $CD3^-$ NK cells. NK effector functions were further assessed by a cytotoxicity assay performed using whole-bulk PBMCs at an effector to target ratio of 20:1 using K562 cells previously labeled by Vybrant DiO Dye (Thermo Fisher Scientific). The cytotoxic capacity of the NK cells was determined after 6 hours coincubation by measuring the percentage of PI^+/DiO dye^+ K562 target cells by flow cytometry taking into account nonspecific K562 cell death.

Multiplex cytokine measurements

Serum samples before and during treatment were used. NK and T-cell cytokines were measured by a flow cytometry bead assay that allows measurement of 13 cytokines (LEGENDplex; BioLegend). Binding of cytokines to the beads was measured using a Fortessa II analyzer (BD Biosciences).

HLA-F IHC

Tissue sections from patients were analyzed by IHC for HLA-F expression. Paraffin sections were incubated with a monoclonal rabbit anti-human HLA-F IgG (Abcam, clone EPR6803).

Data availability

Raw and processed RNA sequencing data from our discovery cohort are deposited on GEO under accession number GSE111414. The other datasets used were accessed upon request through the responsible institutions: TracerX cohort through EGA accession number EGAD00001003206; Rizvi confirmation cohort through dbGaP accession number phs000980.v1.p1.

Statistical analysis

We used multivariable Cox regression models to investigate the association between *KIR3DS1/L1* status and progression-free survival (PFS) adjusted for age and smoking status in the pooled analysis (discovery and confirmation cohort). An additional sensitivity analysis was conducted on the discovery cohort with PD-L1 in the model (considering expression levels of 0%, 1%–50%, and >50%). All analyses were conducted on complete cases, no techniques for multiple imputations were applied. We used the statistical program R (version 3.4.3) for all multivariable analyses and creating the Kaplan–Meier plots. GraphPad Prism version 6.05 was used for statistical analysis of flow cytometry data. All reported *P* values are two-sided and considered exploratory.

Results

Minimal cellular changes in peripheral blood of patients with NSCLC undergoing PD-1–blocking antibody therapy

PBMCs and serum samples were collected from 35 patients with NSCLC immediately before and after two cycles (week 4) of treatment with nivolumab (Table 1). All patients had progressed on or after at least one prior platinum-containing chemotherapy

Published OnlineFirst February 14, 2019; DOI: 10.1158/1078-0432.CCR-18-3041

Table 1. Characteristics of patients with NSCLC in the discovery cohort[a]

Characteristics	Discovery cohort (*N* = 35)
Median age, year (range)	62 (35–83)
Male sex, *n* (%)	20 (57.1)
Histology, *n* (%)	
Adenocarcinoma	26 (74.3)
Squamous cell carcinoma	5 (14.3)
Large cell carcinoma	1 (2.9)
NOS	3 (8.5)
Smoking history, *n* (%)	
Never	7 (20)
Former	14 (40)
Current	14 (40)
Molecular markers, *n* (%)	
No markers detected	22 (62.8)
KRAS mutation	9 (25.6)
EGFR mutation	1 (2.9)
ALK translocation	1 (2.9)
MET exon 14 deletion	1 (2.9)
HER2 mutation	1 (2.9)
Previous therapy lines, *n* (%)	
1	33 (84.6)
2	3 (7.7)
>2	3 (7.7)
ECOG PS, *n* (%)	
0	9 (25.7)
1	18 (51.4)
2	7 (20)
3	1 (3)

Abbreviations: ALK, anaplastic lymphoma kinase; NOS, not otherwise specified.
[a]Patients all received nivolumab monotherapy for at least 3 cycles.

regimen. Median age was 62 years, 42.9% of patients were female, 14.3% had squamous cell histology, and 74.3% adenocarcinoma histology (Table 1). Eastern Cooperative Oncology Group (ECOG) performance status (PS) was 0 or 1 in 77.1% of patients.

Changes in immune cells in the peripheral blood were analyzed in 19 patients with available serial samples. After two cycles of treatment, there were no significant changes in numbers of $CD8^+$ and $CD4^+$ T cells during treatment (Fig. 1A), but a slight increase in $CD4^+$ $CD25^+$ $FoxP3^+$ regulatory T cells was seen (Fig. 1A). No changes were observed in $CD56^+$ $CD3^-$ NK-cell numbers or naïve T cells ($CD45RA^+$ $CCR7^+$ T cells; Fig. 1A). Because $CD8^+$ T cells are considered the main effectors of checkpoint blockade and cancer immunotherapies (1, 2), we analyzed differentially expressed genes in peripheral $CD8^+$ T cells before and during treatment in 5 patients with PR and 5 patients with primary progressive disease to identify mechanisms of resistance to PD-1 therapy (Supplementary Table S1). Messenger-RNA sequencing revealed alterations in very few genes in total peripheral $CD8^+$ T cells during treatment (Supplementary Table S2). Only one gene, the gene for the killer immunoglobulin-like receptor *KIR3DS1*, was clearly differently expressed between responders and nonresponders (Fig. 1B).

Association of *KIR3DS1* genetic variant with resistance to PD-1 blockade

KIRs are a polymorphic family of NK-cell receptors that bind to HLAs (20, 21). The gene product of *KIR3DS1* is an activating variant of the inhibitory KIR3DL1 receptor that binds to Bw4 epitope–containing HLAs (20, 21). The *KIR3DS1* allele was present in the germline of 4 of 5 patients with primary progressive disease and 0 of 5 patients with PR, prompting us to study the allelic variant in the full cohort.

Genotyping of the discovery cohort ($n = 35$) revealed that 15 (42.9%) patients carried the *KIR3DS1* variant while 20 (57.1%) were homozygous for *KIR3DL1*. The whole cohort had an overall response rate of 22.8% (8/35) and a PFS of 2.4 months (Supplementary Fig. S1A). No patient was homozygous for *KIR3DS1* in our cohort. Clinical characteristics were similar between these two groups (Table 2). Thirteen of 17 (76.5%) patients with primary progression carried the activating receptor *KIR3DS1* compared with 2 of 10 (20%) of patients with PR ($P = 0.007$). Patients with the *KIR3DS1* allele present had a significantly higher chance for disease progression (Fig. 1C). The overall response rate (ORR) in patients homozygous for the *KIR3DL1* allele was 40% [7/20 PR, 35%; 1/20 complete response (CR), 5%]. In contrast, the response rate in patients with the *KIR3DS1* allele was 0% ($P = 0.01$). PFS to PD-1 blockade was also worse in patients carrying the *KIR3DS1* allele [Fig. 1E; HR, 2.68; 95% confidence interval (CI), 1.58–4.61; $P = 0.02$]. Patients carrying either the *KIR3DS1* allele or carrying no allele for Bw4-containing *HLAs* showed a lower risk of progression compared with patients carrying *KIR3DS1* alone, but the consideration of Bw4-containing *HLA*s (ligands for KIR3DL1) did not better discriminate between progressing and nonprogressing patients (Supplementary Fig. S1B and S1C). In addition, the PFS of prior chemotherapy regimen did not differ between patients with or without the *KIR3DS1* allele (Supplementary Fig. S2A; HR, 0.80; 95% CI, 0.41–1.55; $P = 0.50$).

We next explored two cohorts of patients with metastatic NSCLC treated with PD-(L)1–blocking antibodies as confirmation cohorts. First, we analyzed a cohort of 34 patients with metastatic NSCLC treated with pembrolizumab (Rizvi confirmation cohort). We selected this cohort because whole-exome sequencing data were available (12). Seven of 13 patients with primary progression carried the allele for the activating receptor *KIR3DS1* compared with 1 of 12 of patients with PR ($P = 0.03$). All other responders (11 of 12) were homozygous for *KIR3DL1*. In this cohort, the response rate in the patients with *KIR3DS1* was 9.1% (1/11) and without *KIR3DS1* 47.8% (11/23). Similarly, PFS to PD-1 blockade was worse in patients carrying the *KIR3DS1* allele (Fig. 2A; HR, 2.64; 95% CI, 1.58–4.61; $P = 0.01$). KIR types in this cohort were determined by a new bioinformatics algorithm that has been developed by us and successfully validated in an independent cohort (TracerX) against a well-characterized published method (19). In addition, we examined by PCR the presence for *KIR3DS1* of another new cohort of 66 patients with metastatic NSCLC that received a PD-(L)1 inhibitor (St. Gallen confirmation cohort). There was a trend with a median time-to-progression of 5.1 months in the *KIR3DS1*-positive group versus 10.2 months in the *KIR3DS1*-negative group. Yet, we did not observe a statistically significant difference of the PFS in this cohort (Fig. 2B; HR, 1.37; 95% CI, 0.69–2.70; $P = 0.36$). In this cohort, the response rate in the patients with *KIR3DS1* was 7.1% (2/28) and 21.1% (8/38) without *KIR3DS1*. The ORR of this cohort is lower than would be expected in such a treatment group (15.1%). This could be a possible explanation for the lack effect in this independent group alone. Unlike in the discovery cohort, *KIR3DS1* homozygous patients were found in the confirmation cohorts (2 in the Rizvi cohort, 4 in the St. Gallen cohort).

Univariate analysis of PFS of the combined cohorts (discovery cohort and the two confirmation cohorts) confirms a significantly worse outcome when *KIR3DS1* was present with a median PFS of only 2.6 months compared with 6.3 months

Published OnlineFirst February 14, 2019; DOI: 10.1158/1078-0432.CCR-18-3041

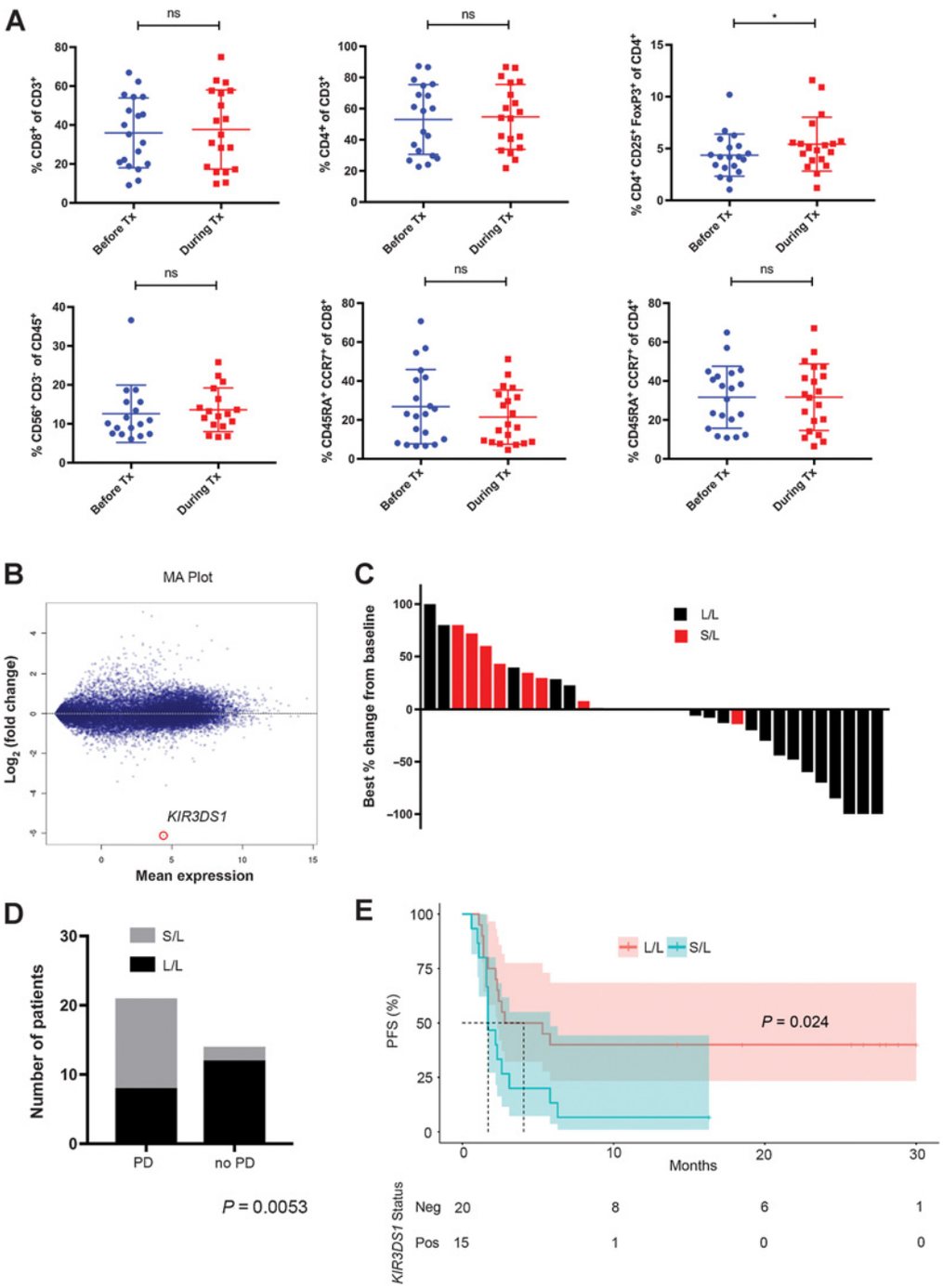

Figure 1.

Presence of KIR3DS1 polymorphism is associated with resistance to PD-1 blockade. **A,** Frequency of peripheral $CD8^+$ T cells, $CD4^+$ T cells, regulatory $CD4^+$ $CD25^+$ $FoxP3^+$ T cells, NK ($CD56^+$ $CD3^-$) cells, naïve $CD8^+$ T cells, and naïve $CD4^+$ T cells in the peripheral blood of patients with NSCLC undergoing PD-1–blocking treatment (Tx) with nivolumab determined by flow cytometry, $N = 19$, *, $P < 0.05$ by paired Student *t* test. Data represented as mean ± SD. **B,** MA plot of the expression analysis in patients responding to PD-1 blockade versus patients not responding. **C,** Best radiographic response determined by RECIST in patients with NSCLC treated with nivolumab. Response assessment was performed in homozygous *KIR3DL1* (L/L) and heterozygous *KIR3DS1/L1* (S/L) patients. **D,** Number of patients with NSCLC in the discovery cohort with the *KIR3DS1* allele present or absent that have progressive disease (PD) or not progressive disease (no PD) in the discovery cohort. Fisher exact test was used for statistical analysis. **E,** PFS of discovery cohort ($N = 35$), according to *KIR3DS1* status. Statistical analysis by Wilcoxon signed-rank test.

Published OnlineFirst February 14, 2019; DOI: 10.1158/1078-0432.CCR-18-3041

Table 2. Patient characteristics of the discovery cohort, according to *KIR3DS1/L1* status

Characteristic	*KIR3DL1/L1* (*N* = 20)	*KIR3DS1/L1* (*N* = 15)	*P*
Median age, year (range)	61 (49–83)	61 (35–75)	0.43[a]
Male sex, *n* (%)	10 (50)	11 (73.3)	0.30[b]
Histology, *n* (%)			
Nonsquamous	17 (85)	13 (86.6)	>0.99[b]
Squamous	3 (15)	2 (13.4)	
Smoking history, *n* (%)			
Yes	17 (85)	11 (73.3)	0.43[b]
No	3 (15)	4 (26.7)	
ECOG status, *n* (%)			
0–1	15 (75)	12 (80)	>0.99[b]
2–3	5 (15)	3 (20)	
PD-L1 status, *n* (%)			
Negative	6 (30)	8 (53.3)	0.11[c]
1–50%	5 (25)	2 (13.4)	
>50%	5 (25)	0 (0)	
Missing	4 (20)	5 (33.3)	

[a]Student *t* test.
[b]Fisher exact test.
[c]χ^2 test.

(Supplementary Fig. S3; Supplementary Table S5; HR, 1.89; 95% CI, 1.24–2.87; $P = 0.0029$). Multivariate analysis considering age and smoking status demonstrated a significantly increased risk of progression in patients with the *KIR3DS1* allele (Supplementary Table S6; HR, 1.91; 95% CI, 1.25–2.91; $P = 0.0027$). When a multivariate analysis was performed that included tumor PD-L1 status considering three groups of expression (0%, 1%–50%, and >50%), the significant effect of the *KIR3DS1* status on the PFS remained (Supplementary Table S7; HR, 1.72; 95% CI, 1.10–2.68; $P = 0.017$). In contrast to this finding, among patients ($n = 99$) with early-stage NSCLCs who were not treated with immunotherapy (TracerX cohort), there was no difference in disease-free survival according to *KIR3DS1* status (Supplementary Fig. S2B; HR, 1.41; 95% CI, 0.58–3.24; $P = 0.44$). We could not observe an association between PD-L1 expression and the *KIR3DS1* status (Table 3). We could also not observe an association with the TMB of patients that had TMB data available (Table 3).

Table 3. Association of PD-L1 status and TMB of pooled cohort

KIR3DS1 status	L/L	S/L or S/S	*P*
PD-L1 status, *n* (%)			
0%	23 (36)	17 (39.5)	0.92[a]
1–50%	18 (28)	12 (27.9)	
>50%	23 (36)	14 (32.6)	
TMB, *n* (%)			
Low (0–11 mutations/Mb)	13 (39.4)	9 (60)	0.22[b]
High (>11 mutations/Mb)	20 (60.6)	6 (40)	

[a]χ^2 test.
[b]Fisher exact test.

The KIR3DS1 receptor associates NK cells with resistance to immune checkpoint blockade

To provide mechanistic insights into the association of KIR3DS1 expression and immune checkpoint blockade resistance, we determined the expression of KIR3DS1 on peripheral immune cells by flow cytometry. KIR3DS1/L1 was mainly expressed on NK cells compared with $CD8^+$ T cells both in the peripheral blood and in the tumor (Fig. 3A). Both *KIR3DL1/L1* and *KIR3DS1/L1* patients showed similar NK-cell numbers and expression of PD-1, CD56 (NCAM1), TBET (TBX21), EOMES, and KI67 in NK cells (Supplementary Fig. S4). PD-1 expression on peripheral NK cells was very low, but higher and significantly decreased upon treatment in patients homozygous for *KIR3DL1*. TIM-3 (HAVcr-2) was higher before treatment in *KIR3DL1/L1* patients compared with *KIR3DS1/L1* patients (Supplementary Fig. S4F). Expression of other inhibitory and activating receptors on NK cells remained unchanged during treatment (Supplementary Fig. S4).

To test the functional potential of NK cells in patients treated with PD-1 blockade, we incubated peripheral NK cells with K562 target cells and analyzed degranulation by CD107a surface staining and production of intracellular cytokines. Patients homozygous for *KIR3DL1* showed increased cytokine production after PD-1 blockade monotherapy compared with those carrying the *KIR3DS1* allele (Fig. 3B; Supplementary Fig. S5A). Similarly, more *KIR3DL1/L1* patients had an increase in tumor cell killing (63%) during treatment compared with patients carrying the *KIR3DS1*

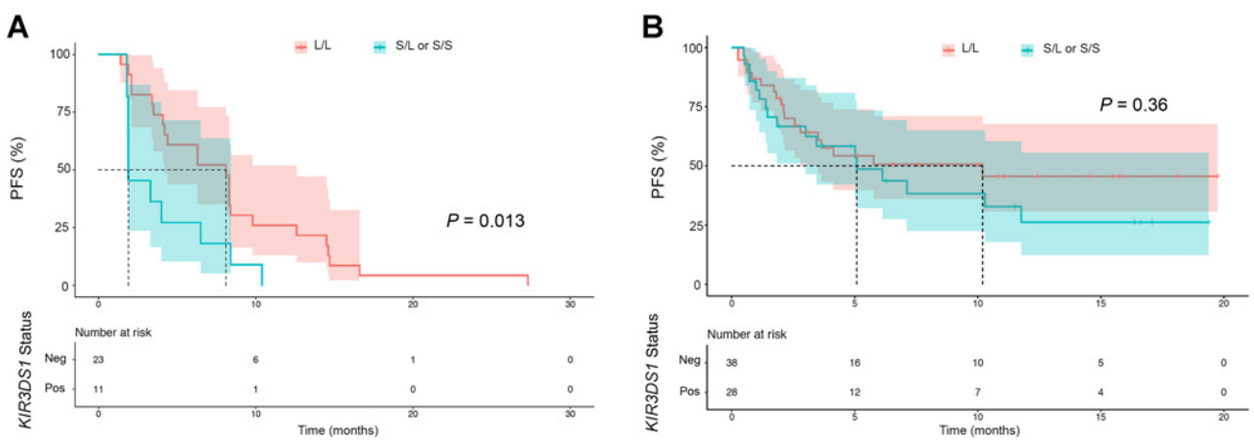

Figure 2.
KIR3DS1 association with PFS in NSCLC checkpoint inhibitor confirmation cohorts. **A,** PFS of confirmation cohort according to *KIR3DS1* status ($N = 34$) from Rizvi and colleagues. Statistical analysis by Wilcoxon signed-rank test. **B,** PFS of confirmation cohort according to *KIR3DS1* status ($N = 66$) of an additional cohort from the cantonal hospital in St. Gallen. Statistical analysis by Wilcoxon signed-rank test.

Published OnlineFirst February 14, 2019; DOI: 10.1158/1078-0432.CCR-18-3041

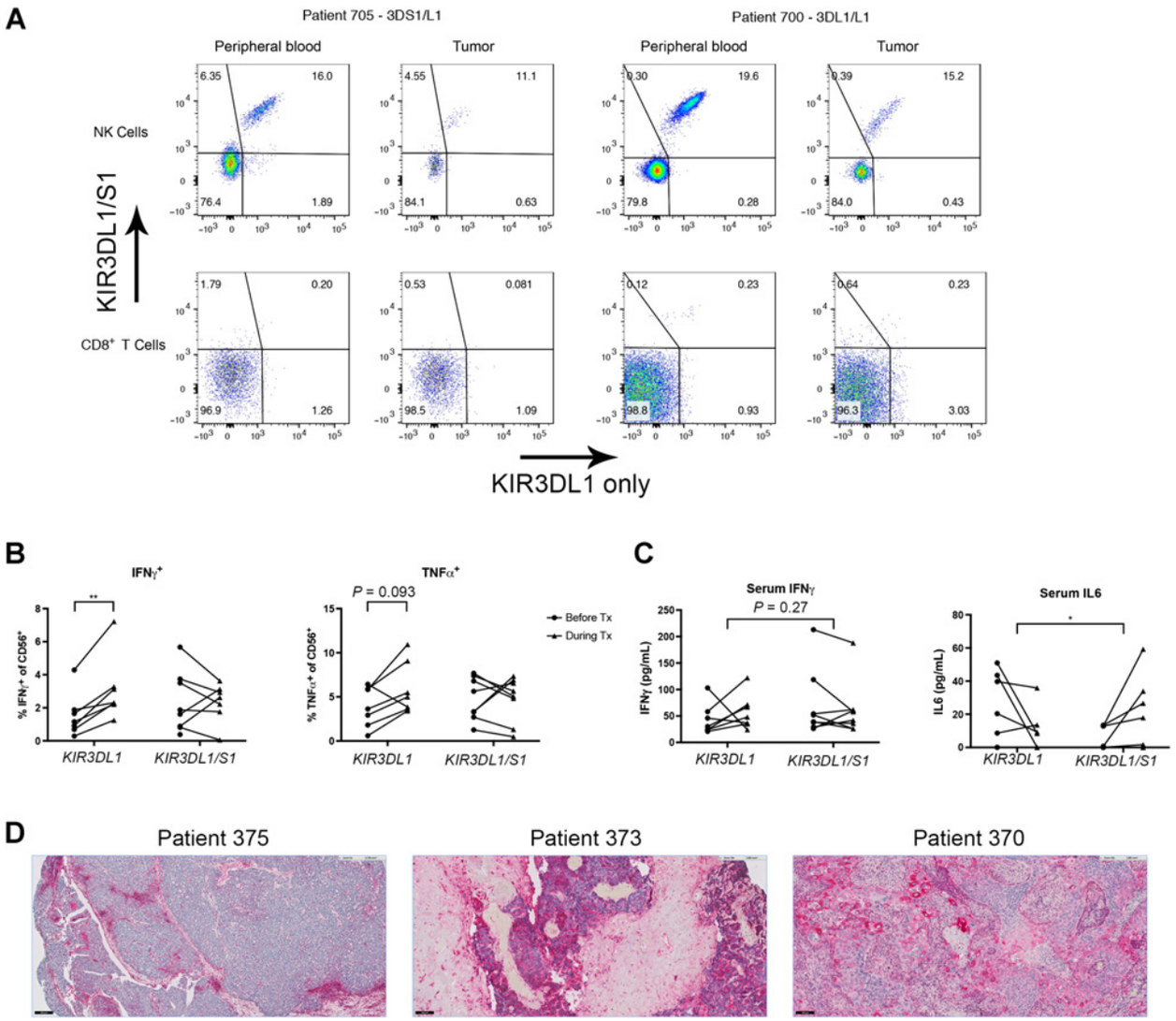

Figure 3.

KIR3DS1 on NK cells is involved in the association with resistance to PD-1 blockade. **A,** Two representative flow cytometric analyses of peripheral and intratumoral NK cells and CD8$^+$ T cells for KIR3DL1 and KIR3DS1 (*y*-axis, antibody that recognizes both KIR3DS1 and KIR3DL1; *x*-axis, antibody that recognizes only KIR3DL1). **B,** Functional analysis of peripheral NK cells before and during treatment with PD-1 blockade. Peripheral NK cells were incubated with K562 target cells, and intracellular cytokine production was determined by flow cytometry. $N = 7$; **, $P < 0.01$ by paired two-way ANOVA with Sidak multiple comparison testing. **C,** Changes of IFNγ and IL6 in the peripheral sera of patients with NSCLC during PD-1 blockade therapy. $N = 7$; *, $P < 0.05$ for the interaction between genotype and treatment by paired two-way ANOVA with Sidak multiple comparison testing. **D,** Representative images of HLA-F staining for NSCLC tissue by IHC in red coloring (bars, 100 μm).

allele (28%) (Supplementary Fig. S5B). Multiplex analysis of NK and T-cell cytokines in the peripheral blood showed a tendency toward reduced IFNγ and significantly increased IL6 levels in patients with NSCLC with *KIR3DS1/L1* heterozygosity (Fig. 3C). There were no significant changes of peripheral T cells depending on the *KIR3DS1* status (Supplementary Fig. S5C–S5H). The presence of activating ligands for KIR3DS1 could lead to continuous stimulation of NK cells and potential NK-cell exhaustion. We therefore stained available tissue for the KIR3DS1 ligand HLA-F. Indeed, several tumors showed a clear positivity for HLA-F IHC staining (Fig. 3D; Supplementary Fig. S6; Supplementary Table S8). In general, most NSCLC samples demonstrated an intermediate to high staining score suggesting that HLA-F upregulation in lung tumors is a common phenomenon (Supplementary Fig. S6; Supplementary Table S8).

Discussion

We identified a receptor gene variation, which is known to modulate NK-cell activation, being associated with worse clinical outcome in patients with metastatic NSCLC treated with PD-1 blockade. We confirmed our findings in a combined analysis of cohorts of patients with metastatic NSCLC treated with PD-(L)1–blocking antibodies. We also show that the genetic

Published OnlineFirst February 14, 2019; DOI: 10.1158/1078-0432.CCR-18-3041

variation is not associated with prognosis in patients with localized NSCLC after resection (TracerX) cohort. In general, *KIR3DS1* seems to be rather a predictive marker for PD-(L)1 therapy than a prognostic marker, although further studies including prospective trials would be needed to definitively answer this question.

The *KIR3DS1/L1* genetic variation has been previously linked to the outcome of treated patients with cancer (22–25). In one study, the presence of the *KIR3DS1* allele predicted increased risk of progression in patients receiving autologous stem cell transplantation for multiple myeloma (24). In another study, the *KIR3DL1/S1* status was associated with outcomes in patients with neuroblastoma treated with anti-GD2 mAb (23). Recent mechanistic studies in a humanized mouse model have shown that the presence of inhibitory KIR3DL1 and Bw4-containing HLA ligands can educate NK cells to be more responsive to the loss of MHC-I molecules on tumor cells (26).

We have identified the *KIR3DS1* allele to be associated with resistance to PD-1 blockade by expression analysis in peripheral $CD8^+$ T cells. Although expression was different between responders and nonresponders on a transcript level, only minimal protein expression was found by flow cytometry on $CD8^+$ T cells compared with NK cells. We therefore focused further analysis on NK cells. NK-cell education describes a process by which the chronic interaction of inhibitory KIRs (e.g., KIR3DL1) with their MHC ligands (e.g., Bw4) promotes NK-cell responsiveness through yet unknown mechanisms (27–29). Our correlative analysis suggests that NK cells are involved in the mechanism of KIR3DS1-associated resistance to PD-1 blockade, because KIR3DL1 or KIR3DS1 were only minimally expressed on peripheral and intratumoral T cells. NK-cell education mediated by KIR3DL1-Bw4 ligation seems unlikely to be the primary cause of resistance, because the predictive value of *KIR3DS1* was reduced when the Bw4 ligands were considered. Thus, the presence or absence of KIR3DL1-binding Bw4-containing HLAs does not improve the discrimination between responders and nonresponders in patients homozygous for *KIR3DL1* (Supplementary Fig S1B). In addition, differences in peripheral NK-cell functionality were only observed after initiation of PD-1 blockade and not prior treatment, which should also be different if education was involved.

Recent analysis of *HLA* types and response to immune checkpoint inhibitors suggests an association with certain *HLA-B* types, mainly linked to presentation capacities of specific *HLA-B* types (30). It is possible that these *HLA* types also associate with differences in NK functionality, which would need further investigation in larger cohorts given the vast numbers of possible combinations. Another possible underlying mechanism might be the induction of dysfunctional or "exhausted" NK cells by continuous KIR3DS1 stimulation by its ligand HLA-F, which was found to be highly expressed in lung cancer (31). Indeed, we confirmed strong expression of HLA-F in selected patients, although this could not be performed in all patients due to unavailability of tumor tissue. Yet, we currently lack a deeper mechanistic understanding of the cellular network that mediates resistance in patients expressing KIR3DS1. Complex human *in vitro* systems or humanized mouse models would be required for functional studies, as *KIR* receptors and *HLAs* both are very weakly conserved between mice and humans. In addition, larger prospective trials are needed to validate the presence of *KIR3DS1* as predictive marker for primary resistance in tumors other than lung cancer and combination treatments such as PD-1/CTLA-4 blockade.

Our results support the hypothesis that NK cells are involved in resistance to PD-1 blockade. NK cells have been known to be important players in the immunosurveillance of cancers and recent efforts have led to the development of checkpoint inhibitors that target inhibitory receptors on NK cells for cancer immunotherapy (21, 32). Lirilumab, for example, targets the immunoglobulin-like domain 2 (2D) of KIR2DL1, 2 and 3, which is engaged by HLA-C epitopes (21, 32). Our findings suggest that NK cells play an important role in mediating the effect of PD-1 blocking immunotherapy. It is conceivable that cross-talk between NK cells and the tumor microenvironment, rather than an independent effect of NK cells, could be responsible for our observations. Indeed, a recent publication described the interaction of NK cells with dendritic cells within the tumor to induce a PD-1 checkpoint inhibitor–responsive microenvironment (10). A recent analysis in a mouse model has additionally provided evidence that NK cells dictate the infiltration of classical dendritic cells into tumors and thereby play an important role in antitumor immunity (33).

In summary, we provide evidence that the *KIR3DS1* genetic variant is associated with the outcome in patients with NSCLC treated with PD-1–directed immunotherapy (summarized in Supplementary Fig. S7). Our findings suggest an important role of NK cells to modulate the therapeutic efficacy of PD-(L)1–targeted therapies. As NK-cell–targeted therapies are available, they might be particularly useful in patients with the *KIR3DS1* allele present. Thus, it will be of utmost clinical relevance to dissect the cellular mechanisms how NK cells interact with other immune effectors in the tumor microenvironment.

Disclosure of Potential Conflicts of Interest

S.I. Rothschild is a consultant/advisory board member for Bristol-Myers Squibb, MSD, AstraZeneca, and Roche. P. Jermann reports receiving commercial research grants from Bristol-Myers Squibb, and reports receiving other commercial research support from Thermo Fisher Scientific. I. Alborelli reports receiving commercial research grants from Bristol-Myers Squibb, and reports receiving other commercial research support from Thermo Fisher Scientific. F. Stenner is a consultant/advisory board member for Bristol-Myers Squibb. Z. Trajanoski reports receiving speakers bureau honoraria from Merck and Roche. H. Läubli reports receiving commercial research grants from Bristol-Myers Squibb and is a consultant/advisory board member for Palleon Pharmaceuticals. No potential conflicts of interest were disclosed by the other authors.

Authors' Contributions

Conception and design: S.I. Rothschild, A. Zippelius, H. Läubli

Development of methodology: M.P. Trefny, F. Uhlenbrock, D. Rieder, A. Zippelius, H. Läubli

Acquisition of data (provided animals, acquired and managed patients, provided facilities, etc.): M.P. Trefny, S.I. Rothschild, F. Uhlenbrock, M. Kaiser, P. Herzig, S. Poechtrager, D.S. Thommen, S. Savic, P. Jermann, I. Alborelli, S. Schaub, F. Stenner, M. Früh, K.D. Mertz, H. Läubli

Analysis and interpretation of data (e.g., statistical analysis, biostatistics, computational analysis): M.P. Trefny, S.I. Rothschild, F. Uhlenbrock, D. Rieder, B. Kasenda, M.A. Stanczak, F. Berner, A.S. Kashyap, M. Kaiser, P. Herzig, D.S. Thommen, F. Geier, P. Jermann, I. Alborelli, M. Früh, Z. Trajanoski, A. Zippelius, H. Läubli

Writing, review, and/or revision of the manuscript: M.P. Trefny, S.I. Rothschild, D. Rieder, B. Kasenda, M.A. Stanczak, F. Berner, A.S. Kashyap, S. Savic, F. Stenner, M. Früh, Z. Trajanoski, K.D. Mertz, A. Zippelius, H. Läubli

Administrative, technical, or material support (i.e., reporting or organizing data, constructing databases): D. Rieder, P. Herzig, S. Poechtrager, S. Savic, L. Flatz, K.D. Mertz, A. Zippelius,
Study supervision: S.I. Rothschild, A. Zippelius, H. Läubli

Acknowledgments

The authors thank Priska Auf der Maur (University and University Hospital of Basel, Basel, Switzerland) for designing the graphical summary. The authors thank the sciCORE (http://scicore.unibas.ch/) scientific computing core facility at University of Basel (Basel, Switzerland) for helping to perform calculations. The authors acknowledge the CRUK TracerX consortium for providing access to the sequencing data of patients undergoing chemotherapy, and Jamie Ashman (Prism Ideas) for editorial assistance in the submission of this manuscript. Most importantly, the authors thank all the patients that allowed the use of their material and made this work possible. H. Läubli was supported by grants from Lichtenstein Foundation, Schoenemakers Foundation, Krebsliga beider Basel, and the Goldschmidt-Jacobson Foundation. A. Zippelius was supported by Krebsforschung Schweiz (KFS-3394-02-2014) and Swiss National Science Foundation (320030_162575).

The costs of publication of this article were defrayed in part by the payment of page charges. This article must therefore be hereby marked *advertisement* in accordance with 18 U.S.C. Section 1734 solely to indicate this fact.

Received September 16, 2018; revised December 14, 2018; accepted February 4, 2019; published first February 14, 2019.

References

1. Chen DS, Mellman I. Elements of cancer immunity and the cancer-immune set point. Nature 2017;541:321–30.
2. Topalian SL, Drake CG, Pardoll DM. Immune checkpoint blockade: a common denominator approach to cancer therapy. Cancer Cell 2015; 27:450–61.
3. Borghaei H, Paz-Ares L, Horn L, Spigel DR, Steins M, Ready NE, et al. Nivolumab versus docetaxel in advanced nonsquamous non-small-cell lung cancer. N Engl J Med 2015;373:1627–39.
4. Brahmer J, Reckamp KL, Baas P, Crino L, Eberhardt WE, Poddubskaya E, et al. Nivolumab versus docetaxel in advanced squamous-cell non-small-cell lung cancer. N Engl J Med 2015;373:123–35.
5. Fehrenbacher L, Spira A, Ballinger M, Kowanetz M, Vansteenkiste J, Mazieres J, et al. Atezolizumab versus docetaxel for patients with previously treated non-small-cell lung cancer (POPLAR): a multicentre, open-label, phase 2 randomised controlled trial. Lancet 2016;387: 1837–46.
6. Herbst RS, Baas P, Kim DW, Felip E, Perez-Gracia JL, Han JY, et al. Pembrolizumab versus docetaxel for previously treated, PD-L1-positive, advanced non-small-cell lung cancer (KEYNOTE-010): a randomised controlled trial. Lancet 2016;387:1540–50.
7. Reck M, Rodriguez-Abreu D, Robinson AG, Hui R, Csoszi T, Fulop A, et al. Pembrolizumab versus chemotherapy for PD-L1-positive non-small-cell lung cancer. N Engl J Med 2016;375:1823–33.
8. Antonia SJ, Villegas A, Daniel D, Vicente D, Murakami S, Hui R, et al. Durvalumab after chemoradiotherapy in stage III non-small-cell lung cancer. N Engl J Med 2017;377:1919–29.
9. Syn NL, Teng MWL, Mok TSK, Soo RA. *De-novo* and acquired resistance to immune checkpoint targeting. Lancet Oncol 2017;18:e731–e41.
10. Barry KC, Hsu J, Broz ML, Cueto FJ, Binnewies M, Combes AJ, et al. A natural killer-dendritic cell axis defines checkpoint therapy-responsive tumor microenvironments. Nat Med 2018;24:1178–91.
11. Parham P, Norman PJ, Abi-Rached L, Guethlein LA. Variable NK cell receptors exemplified by human KIR3DL1/S1. J Immunol 2011;187: 11–9.
12. Rizvi NA, Hellmann MD, Snyder A, Kvistborg P, Makarov V, Havel JJ, et al. Cancer immunology. Mutational landscape determines sensitivity to PD-1 blockade in non-small cell lung cancer. Science 2015;348: 124–8.
13. Jamal-Hanjani M, Wilson GA, McGranahan N, Birkbak NJ, Watkins TBK, Veeriah S, et al. Tracking the evolution of non-small-cell lung cancer. N Engl J Med 2017;376:2109–21.
14. Choppa PC, Vojdani A, Tagle C, Andrin R, Magtoto L. Multiplex PCR for the detection of *Mycoplasma fermentans, M. hominis* and *M. penetrans* in cell cultures and blood samples of patients with chronic fatigue syndrome. Mol Cell Probes 1998;12:301–8.
15. Thommen DS, Schreiner J, Muller P, Herzig P, Roller A, Belousov A, et al. Progression of lung cancer is associated with increased dysfunction of T cells defined by coexpression of multiple inhibitory receptors. Cancer Immunol Res 2015;3:1344–55.
16. Uhrberg M, Valiante NM, Shum BP, Shilling HG, Lienert-Weidenbach K, Corliss B, et al. Human diversity in killer cell inhibitory receptor genes. Immunity 1997;7:753–63.
17. Li H, Handsaker B, Wysoker A, Fennell T, Ruan J, Homer N, et al. The sequence alignment/map format and SAMtools. Bioinformatics 2009;25: 2078–9.
18. Liao Y, Smyth GK, Shi W. featureCounts: an efficient general purpose program for assigning sequence reads to genomic features. Bioinformatics 2014;30:923–30.
19. Norman PJ, Hollenbach JA, Nemat-Gorgani N, Marin WM, Norberg SJ, Ashouri E, et al. Defining KIR and HLA class I genotypes at highest resolution via high-throughput sequencing. Am J Hum Genet 2016;99:375–91.
20. Malmberg KJ, Sohlberg E, Goodridge JP, Ljunggren HG. Immune selection during tumor checkpoint inhibition therapy paves way for NK-cell "missing self" recognition. Immunogenetics 2017;69:547–56.
21. Chiossone L, Vienne M, Kerdiles YM, Vivier E. Natural killer cell immunotherapies against cancer: checkpoint inhibitors and more. Semin Immunol 2017;31:55–63.
22. Boudreau JE, Giglio F, Gooley TA, Stevenson PA, Le Luduec JB, Shaffer BC, et al. KIR3DL1/HL A-B subtypes govern acute myelogenous leukemia relapse after hematopoietic cell transplantation. J Clin Oncol 2017;35: 2268–78.
23. Forlenza CJ, Boudreau JE, Zheng J, Le Luduec JB, Chamberlain E, Heller G, et al. KIR3DL1 allelic polymorphism and HLA-B epitopes modulate response to Anti-GD2 monoclonal antibody in patients with neuroblastoma. J Clin Oncol 2016;34:2443–51.
24. Gabriel IH, Sergeant R, Szydlo R, Apperley JF, DeLavallade H, Alsuliman A, et al. Interaction between KIR3DS1 and HLA-Bw4 predicts for progression-free survival after autologous stem cell transplantation in patients with multiple myeloma. Blood 2010;116:2033–9.
25. Venstrom JM, Pittari G, Gooley TA, Chewning JH, Spellman S, Haagenson M, et al. HLA-C-dependent prevention of leukemia relapse by donor activating KIR2DS1. N Engl J Med 2012;367:805–16.
26. Boudreau JE, Liu XR, Zhao Z, Zhang A, Shultz LD, Greiner DL, et al. Cell-extrinsic MHC class I molecule engagement augments human NK cell education programmed by cell-intrinsic MHC class I. Immunity 2016;45: 280–91.
27. Shifrin N, Raulet DH, Ardolino M. NK cell self tolerance, responsiveness and missing self recognition. Semin Immunol 2014;26:138–44.
28. Raulet DH, Vance RE. Self-tolerance of natural killer cells. Nat Rev Immunol 2006;6:520–31.
29. Elliott JM, Yokoyama WM. Unifying concepts of MHC-dependent natural killer cell education. Trends Immunol 2011;32:364–72.
30. Chowell D, Morris LGT, Grigg CM, Weber JK, Samstein RM, Makarov V, et al. Patient HLA class I genotype influences cancer response to checkpoint blockade immunotherapy. Science 2018;359:582–7.
31. Lin A, Zhang X, Ruan YY, Wang Q, Zhou WJ, Yan WH. HLA-F expression is a prognostic factor in patients with non-small-cell lung cancer. Lung Cancer 2011;74:504–9.
32. Guillerey C, Huntington ND, Smyth MJ. Targeting natural killer cells in cancer immunotherapy. Nat Immunol 2016;17:1025–36.
33. Bottcher JP, Bonavita E, Chakravarty P, Blees H, Cabeza-Cabrerizo M, Sammicheli S, et al. NK cells stimulate recruitment of cDC1 into the tumor microenvironment promoting cancer immune control. Cell 2018;172: 1022–37.

Published OnlineFirst February 14, 2019; DOI: 10.1158/1078-0432.CCR-18-3041

Clinical Cancer Research

A Variant of a Killer Cell Immunoglobulin-like Receptor Is Associated with Resistance to PD-1 Blockade in Lung Cancer

Marcel P. Trefny, Sacha I. Rothschild, Franziska Uhlenbrock, et al.

Clin Cancer Res 2019;25:3026-3034. Published OnlineFirst February 14, 2019.